

Draft: February 2, 2008

Local $u'g'r'i'z'$ Standard Stars in the Chandra Deep Field–South

J. Allyn Smith^{1,2,3}, Douglas L. Tucker^{4,3}, Sahar S. Allam^{5,4}, Christopher T. Rodgers^{1,3}

ABSTRACT

Because several observing programs are underway in various spectral regimes to explore the Chandra Deep Field South (CDF–S), the value of local photometric standards is obvious. As part of an NOAO Surveys Program to establish $u'g'r'i'z'$ standard stars in the southern hemisphere, we have observed the central region of the CDF–S to create local standards for use by other investigators using these filters. As a courtesy, we present the CDF–S standards to the public now, although the main program will not finish until mid-2005.

Subject headings: catalogs — stars: fundamental parameters — standards

1. Introduction

The photometric calibration of the Sloan Digital Sky Survey (SDSS) is based on a relatively new, five-filter, wide-band photometric system ($u'g'r'i'z'$) defined by Fukugita et al. (1996). This system offers three astrophysical advantages over the established Johnson-Cousins $UBVRI$ system: (1) sharper cutoffs of the band edges, (2) minimal overlap of spectral regions between filters, and (3) filter breaks chosen to exclude the strongest night sky emission lines. We note the SDSS z' filter is open on the red end. Therefore, the system transformation coefficients are strongly dependent upon the choice of detector that observers use to match the standard star network.

¹Department of Physics & Astronomy, P.O. Box 3905, University of Wyoming, Laramie, WY 82071

²Current address: Mail Stop D-448; NIS-4, Los Alamos National Laboratory, Los Alamos, NM 87545

³Visiting Astronomer, Cerro Tololo Inter-American Observatory. CTIO is operated by AURA, Inc. under contract to the National Science Foundation.

⁴Fermi National Accelerator Laboratory, MS-127, P.O. Box 500, Batavia, IL 60510

⁵Current address: Astronomy Department, New Mexico State University, Box 30001, Dept. 4500, 1320 Frenger St., Las Cruces, NM 88003

To support the calibration of the SDSS, Smith et al. (2002) developed the $u'g'r'i'z'$ standard star system using the U.S. Naval Observatory– Flagstaff Station 1-m telescope, which is essentially a northern hemisphere and equatorial network. As part of the NOAO Surveys Program,⁶ we have extended our work to establish $u'g'r'i'z'$ standard stars in the southern hemisphere. These new standards are tied to the existing northern and equatorial network (Smith et al. 2002) developed for the SDSS (York et al. 2000).

The Great Observatories Origins Deep Survey (GOODS) (Dickinson & Giavalisco 2002) is a multi-wavelength program which uses the great space-based, and some of the largest ground-based, observatories to obtain deep imaging and spectroscopy of selected fields encompassing both the Hubble Deep Field North and the Chandra Deep Field South (CDF–S). These fields are among the most studied areas in the sky. Several programs are currently underway to probe the CDF–S to an unprecedented depth in several spectral regimes. These include ground-based studies in the optical (e.g. Arnouts et al. 2001; Wolf et al. 2001), and the infrared (e.g. Vandame et al. 2001; Moy et al. 2002); and space-based studies in the X-ray (e.g. Giacconi et al. 2001, 2002; Rosati et al. 2002). Observations of this field are also planned as part of the SIRTf Legacy and HST Treasury Programs, the latter using the new Advanced Camera for Surveys (ACS). This last program, the HST–ACS observations, is baselined to perform $BVi'z'$ imaging (Renzini et al. 2002); hence, $u'g'r'i'z'$ standard stars would be immediately useful to the GOODS observers and others.

Until this report, no one has defined standard stars in the $u'g'r'i'z'$ filter system in or near the CDF–S to use for photometric calibration. As part of our NOAO survey program, we have observed the central region of the CDF–S to create local $u'g'r'i'z'$ standards, presented herein, to facilitate other investigators’ use of these filters. Further, the placement of standard stars within the CDF–S should ensure future observations, facilitating the study of long-term time variable phenomena and transient events in the region.

In this paper, we present details of our observations in §2, we describe the data reductions in §3, and we present the $u'g'r'i'z'$ magnitudes and colors of the CDF–S standard stars in §4. We will examine remaining sources within the CDF–S in a future paper.

2. Observations

For this study we targeted the center of the CDF–S field at J2000 coordinates $\alpha = 03:32:28$, $\delta = -27:48:30$ (Giacconi et al. 2001) [$l = 223.57$; $b = -54.44$]. Due to the nature of

⁶<http://www.noao.edu/gateway/surveys/programs.html>

the SDSS, most of the existing standard stars used to calibrate these CDF–S local standards were on or near the equator. We selected the standard stars used as the basis for this work from the northern and equatorial $u'g'r'i'z'$ network (Smith et al. 2002), since they are currently the only standard stars for this filter system. We may use additional standards being developed by our NOAO Survey Program for future refinement of CDF–S field object magnitudes.

The data were collected with the CTIO 0.9-m telescope using the Tek2k#3 CCD operating at the cassegrain focus. This “Grade-1” CCD is thinned and has an anti-reflection coating, resulting in high quantum efficiency similar to that of the detector used to establish the initial standard system⁷. Observers have used this CCD in a stable configuration on this telescope since October 1995. The imager is controlled by Arcon software (version 3.3) and operated in multiple amplifier read mode. The average gain and read noise values for each of the amplifiers are listed in Table 1. The CCD has 24μ pixels which gives a scale of 0.396 arcsec/pixel and results in a 13.5 arc-minute field of view. We observed with the CTIO SDSS $u'g'r'i'z'$ filter set.

A current, machine-readable version of transmission curves for the CTIO $u'g'r'i'z'$ filter set is not available. For future use, however, we have requested a full spectral transmission scan for this filter set. Likewise, a current machine-readable version of the CCD spectral response is not available. In the meantime, we have generated preliminary response functions for the CTIO-0.9m+Tek2k#3+ $u'g'r'i'z'$ filter system based upon (1) the $u'g'r'i'z'$ filter transmission curves from the manufacturer (Custom Scientific) for an identical filter set, (2) the CTIO Tek2k quantum efficiency from the GIF plot at the CTIO CCD Information website⁸, and the aluminum reflectances from Bennett et al. (1963) as reproduced by Kneale (1994)⁹ (we assume two aluminum reflecting surfaces in the system). Machine-readable tables of these preliminary filter responses are available at our public access URL¹⁰, where updated versions will be posted as new data become available.

In Figure 1 we plot these CTIO-0.9m+Tek2k#3+ $u'g'r'i'z'$ filter system responses and, for comparison, those from the USNO-1.0m+Tek1k+ $u'g'r'i'z'$ filter system used to set up the original $u'g'r'i'z'$ standard star network. The two system responses look quite similar. Given the uncertainties in calculating the CTIO $u'g'r'i'z'$ response function, these curves are

⁷http://www.ctio.noao.edu/ccd_info/ccd_info.html

⁸http://www.ctio.noao.edu/ccd_info/ccd_info.html

⁹<http://www.gemini.edu/documentation/webdocs/spe/spe-te-g0043.pdf>

¹⁰http://www-sdss.fnal.gov:8000/~dtucker/Southern_ugriz/index.html

not inconsistent with the results we report later in this paper (see § 3 below). The values for the instrumental color terms we measure for our CTIO-0.9m data are typically quite small – ranging on average from about 0.02 to 0.06 mag per magnitude in color. (We must emphasize, though, that for the most accurate photometry — i.e., systematic errors less than a few percent — instrumental color terms must be solved for and applied when converting CTIO-0.9m $u'g'r'i'z'$ photometry to the USNO standard system.)

We have examined linearity of the CTIO system using the dome flat lamps on different observing runs and found the response to be stable, linear, and repeatable from 0–62,000 DN. These tests are usually performed once per observing run, weather “permitting.” Figure 2 shows the weighted average of the CCD response as a function of exposure time for three separate linearity sequences taken in May 2002. Figure 3 gives the deviation from linearity by exposure time for the same data. Other tests show identical responses. The full results will be published in the final paper at the end of the program.

We have also examined linearity (and shutter response) by moving a cluster around the detector in a “grid” to look for measurement repeatability. Preliminary results show no significant deviation of derived magnitudes from these tests. The supernovae monitoring group at CTIO has made its shutter timing maps available to us, indicating expected deviations of $\leq 0.12\%$ (1.2 milli-mags) from center to edge of the CCD for our minimum exposure of five seconds. Based on the shutter data obtained by this group, the shutter exposure timing is stable and repeatable.

We collect and median-combine calibration frames daily, usually during the afternoons. These consisted of a minimum of 10 bias and dome flat frames (10 per $g'r'i'z'$ filter). The dome flats were obtained with a color balance filter. Because of a lack of photons, we did not obtain u' dome flats. The dome flat images help us monitor the status of the CCD and look for changes in the flat-field structure. In addition, twilight sky flats were collected in all five filters during one or both of the twilight periods on each observable night. These were median-combined at the end of each observing run to produce a “master” twilight flat and used in the reduction of the data frames. We chose this approach to maintain consistency with the original standard network. At some point during each observing run, we usually collected long dark frames to monitor changes in the hot pixels on the CCD and to look for light leaks. We generated fringe correction frames using the long program object exposures. These were applied to the i' and z' band images.

During a typical night in our standards program, we observe five or six existing standard fields three times each — at the start, near the middle, and at the end of the night — in order to establish an extinction and color term baseline. Between these extended standard sequences, we usually alternate one or two program fields and one to three standard fields.

We use these to monitor the extinction values established by the longer extinction scans. This observing method allows us to maximize the number of target fields while continuously monitoring the atmosphere for changes. Exposure times for the established standard fields ranged from 5 to 240 seconds, with a mean of 7.9 seconds for the shortest exposures (generally the $g'r'i'$ filters).

The program observations — performed under apparently clear conditions on nine different nights spanning three separate observing runs in 2001 September, 2002 February, and 2002 October — consisted of two separate exposure cycles, resulting in eighteen data points per filter. We obtained two additional r' band observations under obviously non-photometric conditions during the September 2001 observing run. These later observations were obtained to use in a differential search for short period variable stars but were not included in the calculations of the final magnitudes. After processing, we determined that our observations from 2002 October 5 were not photometric, so we discarded them from our final calculations of the calibrated magnitudes, leaving a total of sixteen photometric data points per filter. Table 2 lists the circumstances of all our observations of the CDF–S field. The first two columns give the UT and Modified Julian Date (MJD¹¹) of the observation; the third column gives the approximate airmass at the start of the observation sequence. The exposure times (in seconds) for each filter appear in column four, and the last column gives the observer impression and reduction decisions concerning the sky conditions during the observations.

3. Reductions

We performed reductions using version v8.0 of the SDSS software pipeline `mtpipe` (see Tucker et al. 2003), an earlier version of which was used in the setup of the original $u'g'r'i'z'$ standard star network Smith et al. (2002). This pipeline consists of four main packages:

- **preMtFrames**, which creates the directory structure for the reduction of a night’s data, including parameter files needed as input for the other three packages, and runs quality-assurance tests on the raw data.
- **mtFrames**, which processes the images and performs object detection and aperture photometry on target field images. The processing steps include zero subtraction, flat-field and fringe-frame correction.

¹¹The Modified Julian Date is defined by the relation $\text{MJD} \equiv \text{JD} - 2400000.5$, where JD is the Julian Date.

- **excal**, which takes the aperture photometry lists for the standard star target fields (i.e., stars from Smith et al. 2002), identifies the individual standard stars within those fields, and fits the observed raw counts and known $u'g'r'i'z'$ magnitudes to a set of photometric equations to obtain extinction and zero point coefficients. The output from this package allows us to monitor the stability of the night. The default analysis block is three hours, but can be changed as required based upon the data present and upon trends in the reductions. A minimum of ten standard stars are required for the night to be useable.
- **kali**, which applies the fitted photometric equations to the aperture photometry lists of program target fields for the appropriate analysis block (e.g., the CDF–S field).

We note a few small differences between the methods employed in the current reductions and those used in setting up the original $u'g'r'i'z'$ standard star network of Smith et al. (2002). First, since we tailored our current effort towards calibrating standard stars which are typically much fainter than the Smith et al. (2002) standards (which were generally in the range $r' \approx 8 - 12$), we chose a smaller extraction size for our aperture photometry to reduce or minimize the background sky contribution to the noise. For the Smith et al. (2002) standards, we employed a $24''$ -diameter aperture in order to avoid problems associated with defocusing the brightest stars (required for some the observations). In the current program, we have chosen a $14.86''$ -diameter aperture. This smaller aperture reduces the effects of sky noise for the fainter CDF–S target stars; as an added bonus, this size is the one used in the photometric calibration of the SDSS 2.5m data (Gunn et al. 1998; Lupton, Gunn & Szalay 1999; York et al. 2000; Stoughton et al. 2002). Tests on the fainter standards in Smith et al. (2002) show no significant deviations from the published magnitudes using this smaller extraction aperture.

Second, the current version of **mtpipe** uses photometric equations which are slightly modified from the form described in §4.2 of Smith et al. (2002). The photometric equations employed in the current paper are the following:

$$\begin{aligned}
 u'_{\text{inst}} &= u'_o + a_u + k_u X \\
 &\quad + b_u[(u' - g')_o - (u' - g')_{o,zp}] \\
 &\quad + c_u[(u' - g')_o - (u' - g')_{o,zp}][X - X_{zp}] ,
 \end{aligned} \tag{1}$$

$$\begin{aligned}
 g'_{\text{inst}} &= g'_o + a_g + k_g X \\
 &\quad + b_g[(g' - r')_o - (g' - r')_{o,zp}] \\
 &\quad + c_g[(g' - r')_o - (g' - r')_{o,zp}][X - X_{zp}] ,
 \end{aligned} \tag{2}$$

$$\begin{aligned}
 r'_{\text{inst}} &= r'_o + a_r + k_r X \\
 &\quad + b_r[(r' - i')_o - (r' - i')_{o,\text{zp}}] \\
 &\quad + c_r[(r' - i')_o - (r' - i')_{o,\text{zp}}][X - X_{\text{zp}}] ,
 \end{aligned} \tag{3}$$

$$\begin{aligned}
 i'_{\text{inst}} &= i'_o + a_i + k_i X \\
 &\quad + b_i[(i' - z')_o - (i' - z')_{o,\text{zp}}] \\
 &\quad + c_i[(i' - z')_o - (i' - z')_{o,\text{zp}}][X - X_{\text{zp}}] ,
 \end{aligned} \tag{4}$$

$$\begin{aligned}
 z'_{\text{inst}} &= z'_o + a_z + k_z X \\
 &\quad + b_z[(i' - z')_o - (i' - z')_{o,\text{zp}}] \\
 &\quad + c_z[(i' - z')_o - (i' - z')_{o,\text{zp}}][X - X_{\text{zp}}] .
 \end{aligned} \tag{5}$$

Taking the g' equation as an example, we note that g'_{inst} is the measured instrumental magnitude, g'_o is the extra-atmospheric magnitude, $(g' - r')_o$ is the extra-atmospheric color, a_g is the nightly zero point, k_g is the first order extinction coefficient, b_g is the system transform coefficient, c_g is the second order (color) extinction coefficient, and X is the airmass of the observation. The zeropoint constants, X_{zp} and $(g' - r')_{o,\text{zp}}$ were defined, respectively, to be the average standard star observation airmass $\langle X \rangle = 1.3$ and the “cosmic color,” as listed in Table 3 of Smith et al. (2002). Note that the above equations differ from their analogs in Smith et al. (2002) by the inclusion of zeropoint colors in the system transform (“b”) terms. (Note also that there are some differences in the calibration methodology used in the current paper as opposed to that now used in standard photometric calibrations of the SDSS imaging data. In particular, standard SDSS calibrations now use different values for the zeropoint colors; further, standard SDSS calibrations now index the i' filter to $(r' - i')$ and not to $(i' - z')$; for more details see Tucker et al. (2003).)

Third, in Smith et al. (2002), since we used one telescope (the USNO 1-m) for all the observations in setting up the original $u'g'r'i'z'$ standard star network, we set all values of the system transform (“b”) coefficients identically to zero. Here, we are using a different telescope, so we solve for these “b” terms.

Fourth, instead of using the first-order inverse photometric equations to convert from instrumental magnitudes to calibrated magnitudes in **kali** (eqs. 9 – 13 of Smith et al. 2002), the current version of **mtpipe** does this conversion by solving the above equations iteratively.

Finally, since none of the $(u' - i')$ and $(u' - z')$ colors of the final set of CDF–S standards are very red, no red leak corrections were applied to the CDF–S u' magnitudes.

With these caveats in mind, the night characterization data from **mtpipe** for each of the photometric nights included in this project are given in Table 3. These data include the MJD of observation (column 1), filter (column 2), zero points (column 3), system transformation

terms (column 4), and first-order extinction terms (columns 5 through 7). Note that the zero points and system transformation terms are solved on a night-by-night basis; since it is not uncommon for the first-order extinctions to vary during a night, we typically solve for them in 3-hour-long blocks of time. Finally, columns 8 and 9 give the rms errors for, and numbers of, the standard stars observed that night which were used in the photometric solutions. The weighted mean averages are listed by filter at the bottom of the table as an aid to observers looking for mean site values. In a footnote, we also list the second order extinction terms derived in Smith et al. (2002).

Figure 4 shows the photometric zeropoint versus MJD for each filter. We see the slight degradation of telescope throughput with time, a result of the mirror not being re-aluminized over the course of this program to date. Figure 5 of Smith et al. (2002) shows similar trends for the USNO-1.0m telescope, but the effect of re-aluminization is clearly seen. Figure 5 shows the first order extinction coefficients for each reduction block by MJD. As shown, all the nights used for these data were well behaved. Finally, Figure 6 shows the residuals of the `excal` solution for each filter by MJD for each of the standard stars used in the photometric solution. The plot is in the sense (observed – true), where “true” comes from Smith et al. (2002). This plot may be slightly misleading since we did night-by-night solutions rather than a global solution.

At this point in the reduction process using `mtpipe`, we had sixteen calibrated object lists for the CDF–S, one list for each of the sixteen photometric exposures of this field. We combined these lists by taking the (unweighted) mean magnitude of each object in each filter. To avoid problems associated with signal-to-noise mismatches between the long and the short exposures, we only included in the mean magnitudes those measurements having photon noise errors of ≤ 0.05 mag. We excluded saturated measurements from the mean magnitude calculations. The resulting list of candidate CDF–S standards contains 355 objects.

We culled this list using the following criteria:

- The mean magnitude in r' must have been derived from at least ten good individual measurements.
- The standard deviation of the individual measurements in r' must be less than 0.10 mag (to avoid variables).
- The error in the mean magnitude in r' (standard deviation of the mean) must be less than 0.03 mag (to be useful as a standard star).
- The mean magnitude in r' must be less than 18.0, which is approximately the limit of

our present data to achieve an error in the mean r' magnitude of less than 0.03 mag.

After culling the `mtpipe` output using the above criteria, only 24 objects remained as candidate standard stars. Then, we ran SExtractor (Bertin and Arnouts 1996) on one of our long CDF–S exposures to obtain the automated star-galaxy classifier value. Any object classified as non-stellar either by SExtractor, or by eye, was removed from the list of candidate standards. This resulted in removal of two galaxies. Further, we used the ESO Imaging Survey (EIS) stellar catalog (Groenewegen et al. 2002) to confirm our star-galaxy separation for the brighter objects in our frames, and we deferred to the much deeper EIS catalog classification for our fainter sources. Finally, we performed a coordinate match with the COMBO-17 Survey (Wolf et al. 2001) BVR sources to obtain cross reference designations. The final list presented here contains 22 CDF–S standard stars.

4. The CDF–S Standard Stars

Here, we present the calibrated magnitude and color data for each star in our final list of CDF–S local standards.

Table 4 shows the CDF–S standard stars arranged in order of increasing r' -band magnitude and contains the COMBO-17 designation and the right ascension and declination (J2000) in the first three columns. The next five columns give the r' band magnitudes and four color indices. These five columns are linked with the following five columns (9-13) which give the estimated rms error — i.e., the standard deviation of the mean — of the measurements. As a note, during the reductions we calculated the five filter magnitudes. We report colors here as an observational aid. The associated uncertainties for the colors are derived from the magnitude errors added in quadrature. As such, they may be slightly overestimated, since magnitude errors in different filters tend to be correlated. The last five columns of this table list the number of individual measurements, by filter, that were used to determine the final magnitudes. Finally, Table 5 gives the COMBO-17 and ESO Imaging Survey (EIS) (Arnouts et al. 2001) designations with the coordinates (J2000) for each of the stars in the final standard list. As with Table 4, this list is arranged in order of increasing r' -band magnitude. A finder chart, based upon one of our long r' band images and showing the location of each of these standard stars, appears in Figure 7.

We present a histogram of the distribution of $(g' - r')$ colors of the CDF–S local standards in Figure 8. Figure 9 shows the estimated rms errors (the standard deviation of the mean) in the calibrated magnitudes versus the calibrated magnitude for the CDF–S local standards in each of the five filters. Figure 10 shows the rms errors for the calibrated magnitudes versus

the color for the CDF–S local standards in each of the filters.

We began this effort in September 2000 using the 0.9-m at CTIO and the same observers and reduction software that were used in the setup of the original $u'g'r'i'z'$ standard network described in Smith et al. (2002). We undertook this effort to provide a uniform set of standard stars in the $u'g'r'i'z'$ system across the sky with the goal to provide future investigators a convenient starting grid to establish tertiary standards for their own work, without the need for an extensive end-to-end standardization effort. Observations of this field will continue through the course of our survey program. As they become available, updated magnitudes and colors, along with all of the southern standard stars, will be posted our a public access URL mentioned previously. We estimate that the entire grid of standard star from this project will become available for public dissemination by mid-2005.

We acknowledge the National Optical Astronomy Observatories for the observing time granted through the NOAO Survey Program, the staff at CTIO for its help, especially Edgardo Cosgrove, Arturo Gomaiez, Nick Suntzeff, and Stefanie Wachter. We are grateful to the National Science Foundation for support through AST-0098401. JAS acknowledges Amy Felty and Jeanne Odermann for their careful reading of the manuscript and proper application of the laws of English.

DLT was supported by the US Department of Energy under contract No. DE-AC02-76CH03000.

We thank the anonymous referee for insightful comments which streghened this paper and enhanced the overall presentation of the data. In this vein, we also extend our thanks to all manuscript reviewers for their diligent work.

The EIS data are based on observations carried out using the MPG/ESO 2.2m Telescope and the ESO New Technology Telescope (NTT) at the La Silla observatory under Program-ID No. 164.0-0561.

This research has made use of the SIMBAD database, operated at CDS; the VizieR catalog access tool, CDS; and the Aladin, developed by CDS, Strasbourg, France.

REFERENCES

Arnouts, S., et al. 2001, A&A, 379, 740

Bennett et al. 1963, Journal of the Optical Society of America, 53, 1083

- Bertin, E., & Arnouts, S. 1996, *A&AS*, 117, 393
- Dickinson, M., & Giavalisco, M., et al. 2002, to appear in the Proceedings of the ESO Workshop “The Mass of Galaxies at Low and High Redshift,” eds. R. Bender and A. Renzini (astro-ph/0204213)
- Fukugita, M., Ichikawa, T., Gunn, J. E., Doi, M., Shimasaku, K., & Schneider, D.P. 1996, *AJ*, 111, 1748
- Giacconi, R., et al. 2001, *ApJ*, 551, 624
- Giacconi, R., et al. 2002, *ApJS*, 139, 369
- Groenewegen, M.A.T., et al. 2002, *A&A*, 392, 741
- Gunn, J.E., et al. 1998, *AJ*, 116, 3040
- Kneale, R. 1994, “Functional Specification for the Gemini Coating Plants,” SPE-TE-G0043
- Lupton, R.H., Gunn, J.E., & Szalay, A.S. 1999, *AJ*, 118, 1406
- Moy, E., Barmby, P., Rigopoulou, D., Huang, J.-S., Willner, S.P., & Fazio, G.G. 2002, *A&A*, submitted (astro-ph/0211247).
- Renzini, A., Cesarsky, C., Cristiani, S., da Costa, L., Fosbury, R., Hook, R., Leibundgut, B., Rosati, P., & Vandame, B. 2002, (astro-ph/0204214)
- Rosati, P., et al. 2002 *ApJ*, 566, 667
- Smith, J.A., et al. 2002 *AJ*, 123, 2121
- Stoughton, C., et al. 2002 *AJ*, 123, 485
- Tucker, D.L. et al. 2003 in preparation
- Vandame, B., et al. 2001, *A&A*, submitted (astro-ph/0102300, under revision)
- Wolf, C., Dye, S., Kleinheinrich, M., Meisenheimer, K., Rix, H.-W., & Wisotzki, L. 2001 *A&A*, 377, 442
- York, D.G., et al. 2000 *AJ*, 120, 1579

Table 1. CCD Parameters

Side	Gain (epadu)	Read Noise (e^-)
upper Left	3.1	4.7
lower Left	3.0	5.4
upper Right	3.0	4.6
lower Right	3.0	5.1

Table 2. Observing Circumstances for the CDF-S

YYMMDD	MJD	Airmass	Exposure (sec)					Comments
			r'	g'	u'	i'	z'	
010919	52171	1.04	30	30	240	30	45	Photometric
		1.03	180	180	1440	180	270	Photometric
010920	52172	1.02	30	30	240	30	45	Photometric
		1.02	180	180	1440	180	270	Photometric
010922	52174	...	30	Differential (r' filter only)
		...	180	Differential (r' filter only)
		...	30	Differential (r' filter only)
		...	180	Differential (r' filter only)
020204	52309	1.11	30	30	240	30	45	Photometric
		1.13	180	180	1440	180	270	Photometric
020205	52310	1.17	30	30	240	30	45	Photometric
		1.23	180	180	1440	180	270	Photometric
021005	52552	1.01	20	25	150	20	30	Non-photometric on analysis
		1.00	180	180	1440	180	240	Non-photometric on analysis
021006	52553	1.02	20	25	150	20	30	Photometric
		1.02	180	180	1440	180	240	Photometric
021007	52554	1.02	20	25	150	20	30	Photometric
		1.01	180	180	1440	180	240	Photometric
021010	52557	1.01	20	25	150	20	30	Photometric
		1.01	180	180	1440	180	240	Photometric
021011	52558	1.05	20	25	150	20	30	Photometric
		1.04	100	125	750	100	150	Photometric

Table 3. Night Characterization Coefficients & Averages*

MJD	Filter	Zeropoint (a)	Instr. Color (b)	1st-Order Ext. (k)			Std. rms	# Std.
(1)	(2)	(3)	(4)	block 0 (5)	block 1 (6)	block 2 (7)	(mag) (8)	stars (9)
04:22-09:25 UT								
52171	u'	-20.952±0.020	-0.011±0.010	0.475±0.015	0.018	20
52171	g'	-22.640±0.013	-0.006±0.012	0.184±0.008	0.009	19
52171	r'	-22.605±0.009	-0.137±0.016	0.093±0.005	0.007	27
52171	i'	-22.153±0.011	-0.150±0.025	0.061±0.005	0.006	19
52171	z'	-21.279±0.027	-0.107±0.062	0.050±0.013	0.014	18
23:54-02:54 UT 02:54-05:54 UT 05:54-09:29 UT								
52172	u'	-20.944±0.025	-0.013±0.011	0.449±0.018	0.465±0.019	0.466±0.020	0.020	18
52172	g'	-22.618±0.013	0.049±0.010	0.182±0.009	0.195±0.010	0.183±0.010	0.010	19
52172	r'	-22.582±0.012	0.011±0.020	0.112±0.008	0.114±0.009	0.107±0.009	0.009	19
52172	i'	-22.107±0.015	0.007±0.032	0.060±0.009	0.069±0.010	0.057±0.010	0.010	19
52172	z'	-21.229±0.021	0.018±0.045	0.034±0.013	0.053±0.014	0.036±0.014	0.015	19
00:35-03:35 UT 03:35-09:05 UT ...								
52309	u'	-20.930±0.022	-0.030±0.008	0.480±0.016	0.503±0.014	...	0.017	17
52309	g'	-22.531±0.013	0.055±0.010	0.170±0.009	0.173±0.008	...	0.010	20
52309	r'	-22.513±0.008	-0.062±0.013	0.091±0.006	0.092±0.005	...	0.006	17
52309	i'	-21.988±0.012	0.022±0.026	0.056±0.008	0.054±0.007	...	0.009	20
52309	z'	-21.080±0.015	0.136±0.033	0.059±0.010	0.058±0.009	...	0.011	19
00:44-03:44 UT 03:44-09:14 UT ...								
52310	u'	-20.908±0.013	-0.039±0.005	0.486±0.010	0.463±0.009	...	0.010	11
52310	g'	-22.484±0.008	0.064±0.005	0.162±0.004	0.150±0.005	...	0.005	14
52310	r'	-22.491±0.007	-0.041±0.010	0.090±0.003	0.088±0.004	...	0.004	13
52310	i'	-21.958±0.014	0.037±0.028	0.051±0.007	0.041±0.007	...	0.009	14
52310	z'	-21.073±0.015	0.189±0.027	0.056±0.007	0.059±0.008	...	0.009	14
00:26-03:26 UT 03:26-09:22 UT ...								
52553	u'	-20.757±0.008	-0.018±0.004	0.455±0.006	0.457±0.006	...	0.007	21
52553	g'	-22.458±0.013	0.020±0.011	0.184±0.008	0.176±0.007	...	0.011	26
52553	r'	-22.407±0.011	-0.018±0.020	0.087±0.006	0.082±0.006	...	0.009	27
52553	i'	-21.931±0.013	-0.043±0.029	0.046±0.007	0.034±0.007	...	0.011	27
52553	z'	-21.097±0.012	-0.036±0.028	0.055±0.007	0.040±0.006	...	0.010	27
23:49-02:49 UT 02:49-05:49 UT 05:49-09:25 UT								
52554	u'	-20.828±0.023	-0.025±0.008	0.500±0.018	0.506±0.016	0.496±0.016	0.016	20
52554	g'	-22.485±0.011	0.015±0.008	0.194±0.009	0.189±0.008	0.181±0.008	0.007	18
52554	r'	-22.465±0.015	-0.055±0.022	0.120±0.011	0.114±0.010	0.109±0.010	0.010	22
52554	i'	-21.985±0.018	-0.063±0.040	0.069±0.014	0.054±0.012	0.063±0.012	0.011	22
52554	z'	-21.095±0.015	0.001±0.034	0.039±0.013	0.018±0.010	0.022±0.012	0.009	20
23:46-02:46 UT 02:46-05:46 UT 05:46-08:50 UT								
52557	u'	-20.801±0.032	-0.011±0.006	0.453±0.027	0.509±0.025	0.504±0.026	0.009	13
52557	g'	-22.426±0.026	-0.000±0.012	0.136±0.021	0.150±0.020	0.148±0.020	0.011	15
52557	r'	-22.475±0.022	-0.072±0.020	0.129±0.018	0.129±0.017	0.124±0.016	0.009	17
52557	i'	-22.005±0.025	-0.127±0.033	0.084±0.020	0.080±0.019	0.075±0.019	0.010	16
52557	z'	-21.095±0.025	-0.042±0.030	0.039±0.019	0.053±0.018	0.045±0.018	0.009	15
23:56-02:56 UT 02:56-05:56 UT 05:56-09:25 UT								
52558	u'	-20.818±0.021	-0.000±0.010	0.513±0.015	0.510±0.016	0.498±0.016	0.017	22
52558	g'	-22.454±0.012	-0.009±0.009	0.173±0.007	0.173±0.008	0.169±0.008	0.008	21
52558	r'	-22.440±0.013	-0.153±0.022	0.087±0.007	0.087±0.008	0.082±0.008	0.009	23
52558	i'	-21.940±0.012	-0.041±0.024	0.049±0.006	0.042±0.007	0.045±0.007	0.007	20
52558	z'	-21.048±0.020	0.009±0.043	0.024±0.012	0.018±0.012	0.012±0.013	0.012	23
Ave. u' -20.829±0.006 -0.021±0.002 0.472±0.003								
Ave. g' -22.508±0.004 0.035±0.003 0.172±0.002								
Ave. r' -22.507±0.004 -0.062±0.006 0.093±0.001								
Ave. i' -22.014±0.005 -0.044±0.010 0.052±0.002								
Ave. z' -21.105±0.006 0.041±0.012 0.044±0.002								

*The second order extinction term values are -2.1×10^{-2} , -1.6×10^{-2} , -4.0×10^{-3} , 6.0×10^{-3} and 3.0×10^{-3} , for the u' , g' , r' , i' and z' respectively. These values are set to the determined coefficients from Smith et al. (2002).

Table 4. The $u'g'r'i'z'$ Observations for CDFS Local Standard Stars: Calibrated
Magnitudes and Colors.

COMBO-17 #	RA (2000.0) (2)	DEC (2000.0) (3)	r' (4)	$u' - g'$ (5)	$g' - r'$ (6)	$r' - i'$ (7)	$i' - z'$ (8)	Estimate of rms Mean Error					Number of Observations				
								$\sigma_{r'}$	$\sigma_{u'-g'}$	$\sigma_{g'-r'}$	$\sigma_{r'-i'}$	$\sigma_{i'-z'}$	$n_{u'}$	$n_{g'}$	$n_{r'}$	$n_{i'}$	$n_{z'}$
(1)	(2)	(3)	(4)	(5)	(6)	(7)	(8)	(9)	(10)	(11)	(12)	(13)	(14)	(15)	(16)	(17)	(18)
24094	03 32 24.69	-27 53 59.6	13.550	1.303	0.435	0.147	0.031	0.002	0.004	0.004	0.004	0.004	15	16	16	16	16
34469	03 32 50.42	-27 48 33.1	13.838	1.319	0.435	0.140	0.046	0.001	0.005	0.003	0.003	0.004	16	16	16	16	16
47831	03 32 40.22	-27 42 23.7	13.885	1.803	0.656	0.257	0.112	0.003	0.012	0.006	0.006	0.006	15	16	16	16	16
23984	03 32 04.05	-27 53 54.9	14.640	1.172	0.402	0.137	0.007	0.005	0.015	0.007	0.007	0.008	15	16	16	16	16
38206	03 32 52.34	-27 46 26.0	15.179	2.146	0.866	0.316	0.161	0.003	0.043	0.009	0.005	0.007	15	16	16	16	16
27534	03 32 55.60	-27 51 26.2	15.248	1.497	0.560	0.198	0.084	0.003	0.021	0.006	0.004	0.009	14	14	14	14	14
39797	03 32 10.44	-27 45 06.8	15.308	1.245	0.467	0.172	0.070	0.004	0.023	0.007	0.006	0.010	16	16	16	16	16
46764	03 32 13.77	-27 42 13.6	15.736	1.673	0.818	0.358	0.180	0.009	0.169	0.016	0.013	0.013	11	16	16	16	16
41920	03 32 08.13	-27 44 17.5	15.774	1.045	0.332	0.098	0.039	0.004	0.017	0.008	0.010	0.017	15	16	16	16	16
27876	03 32 55.46	-27 51 06.4	15.873	2.074	1.104	0.490	0.239	0.007	0.089	0.016	0.010	0.009	7	14	14	14	14
20195	03 32 49.63	-27 54 54.0	15.898	1.397	0.564	0.244	0.088	0.010	0.033	0.016	0.013	0.013	13	14	14	13	14
26202	03 32 32.88	-27 51 47.8	16.375	1.006	0.361	0.117	0.057	0.009	0.037	0.013	0.014	0.018	13	14	14	14	13
21659	03 32 54.69	-27 54 01.8	16.445	0.996	1.034	0.975	0.438	0.017	0.115	0.023	0.019	0.014	9	13	14	14	14
44059	03 32 10.22	-27 43 06.9	16.696	2.142	0.802	0.362	0.109	0.015	0.023	0.025	0.021	0.035	3	16	16	16	14
46429	03 32 31.60	-27 42 08.2	17.191	1.550	0.709	0.341	0.212	0.022	0.197	0.045	0.037	0.064	4	14	16	16	14
43791	03 32 40.75	-27 43 18.4	17.329	...	0.815	0.345	0.188	0.019	...	0.041	0.023	0.058	0	11	15	12	7
45812	03 32 33.19	-27 42 21.2	17.345	...	1.087	0.660	0.311	0.017	...	0.034	0.023	0.052	0	11	16	16	11
38427	03 32 06.24	-27 45 42.4	17.424	0.866	0.428	0.219	0.183	0.019	0.225	0.031	0.033	0.089	9	16	16	11	7
35104	03 32 53.42	-27 47 20.4	17.535	...	1.269	0.810	0.420	0.023	...	0.057	0.035	0.035	0	9	16	16	12
30965	03 32 22.34	-27 49 25.3	17.759	1.112	0.992	0.380	0.254	0.020	...	0.026	0.028	0.047	1	8	13	8	6
22486	03 32 10.87	-27 53 29.4	17.814	...	0.736	0.227	0.047	0.027	...	0.037	0.031	...	0	8	12	8	1
21747	03 32 15.96	-27 53 49.9	17.980	...	1.155	0.520	0.321	0.026	...	0.043	0.032	0.105	0	7	10	8	6

Table 5. Designation Cross Reference Table

COMBO-17 #	RA (J2000.0)	DEC (J2000.0)	EIS Reference #
24094	03 32 24.69	-27 53 59.6	J033224.70-275400.1
34469	03 32 50.42	-27 48 33.1	J033250.45-274833.4
47831	03 32 40.22	-27 42 23.7	J033240.26-274224.0
23984	03 32 04.05	-27 53 54.9	J033204.08-275355.1
38206	03 32 52.34	-27 46 26.0	J033252.36-274626.6
27534	03 32 55.60	-27 51 26.2	J033255.63-275126.4
39797	03 32 10.44	-27 45 06.8	J033210.46-274507.5
46764	03 32 13.77	-27 42 13.6	J033213.80-274213.9
41920	03 32 08.13	-27 44 17.5	J033208.16-274417.8
27876	03 32 55.46	-27 51 06.4	J033255.51-275106.6
20195	03 32 49.63	-27 54 54.0	J033249.66-275454.1
26202	03 32 32.88	-27 51 47.8	J033232.88-275148.3
21659	03 32 54.69	-27 54 01.8	J033254.70-275401.8
44059	03 32 10.22	-27 43 06.9	J033210.27-274307.2
46429	03 32 31.60	-27 42 08.2	J033231.64-274208.1
43791	03 32 40.75	-27 43 18.4	J033240.76-274318.6
45812	03 32 33.19	-27 42 21.2	J033233.21-274221.5
38427	03 32 06.24	-27 45 42.4	J033206.26-274542.7
35104	03 32 53.42	-27 47 20.4	J033253.43-274720.8
30965	03 32 22.34	-27 49 25.3	J033222.35-274925.7
22486	03 32 10.87	-27 53 29.4	J033210.88-275329.8
21747	03 32 15.96	-27 53 49.9	J033216.00-275350.2

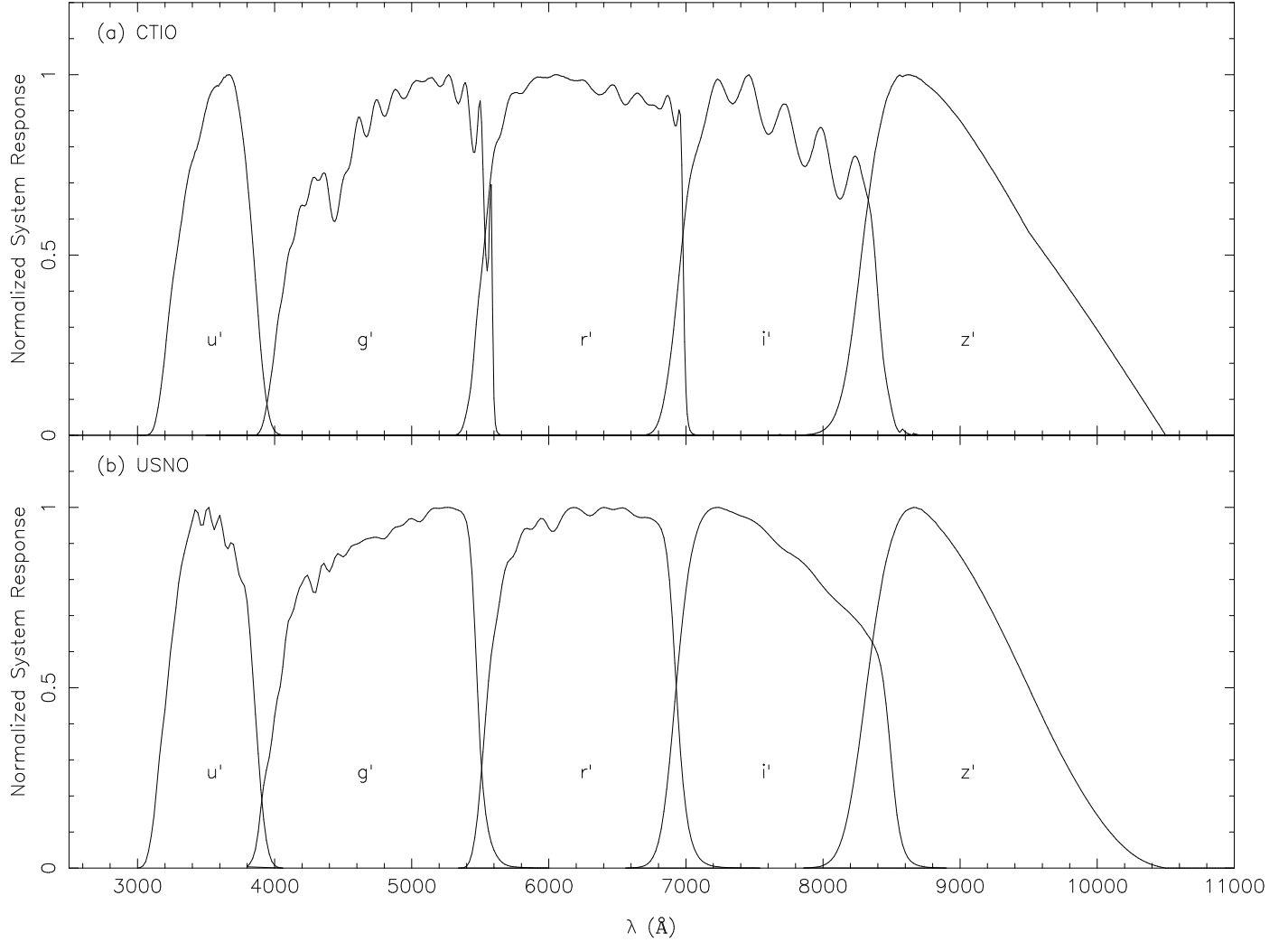


Fig. 1.— The (normalized) responses of the extra-atmospheric $u'g'r'i'z'$ system bandpasses for the (a) CTIO 0.9-m and the (b) USNO 1.0-m telescope systems. The CTIO data should be considered preliminary as the CCD response function was taken from the GIF plot at http://www.ctio.noao.edu/ccd_info/ccd_info.html and is approximately seven years old. The filter data are from the manufacturer for an identical filter set to the one used. Note the similarity between the two systems, supported by the low color term values derived in the paper.

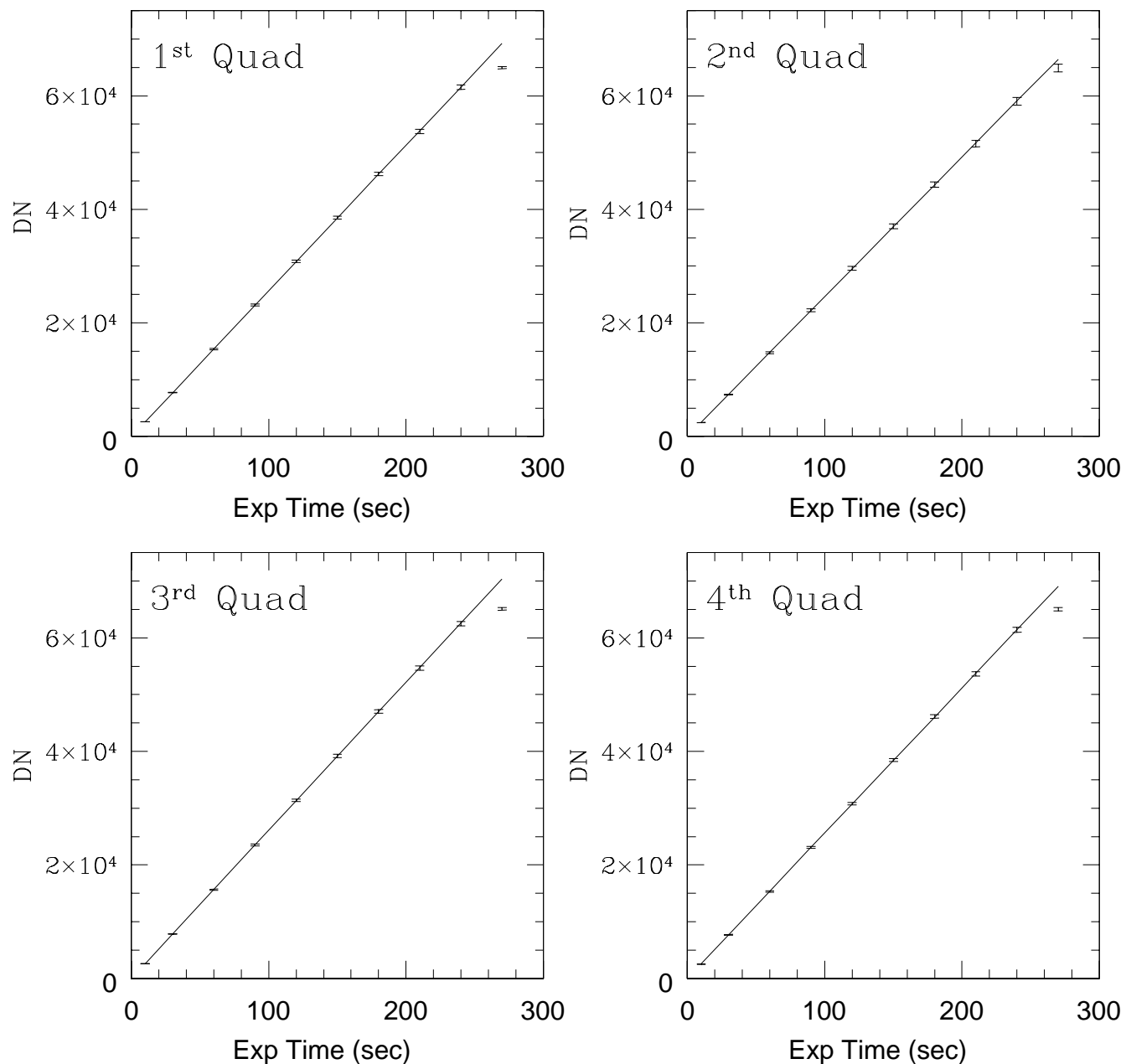


Fig. 2.— Linearity response tests for each quadrant of the Tek2k#3 detector. These show the weighted averages of three independent tests taken during the May 2002 observing run. As labelled, the quadrants refer to: 1=LL; 2=UL; 3=LR; and 4=UR as viewed in the default orientation at the telescope (pixel 0,0 in LL; 2048,2048 in UR).

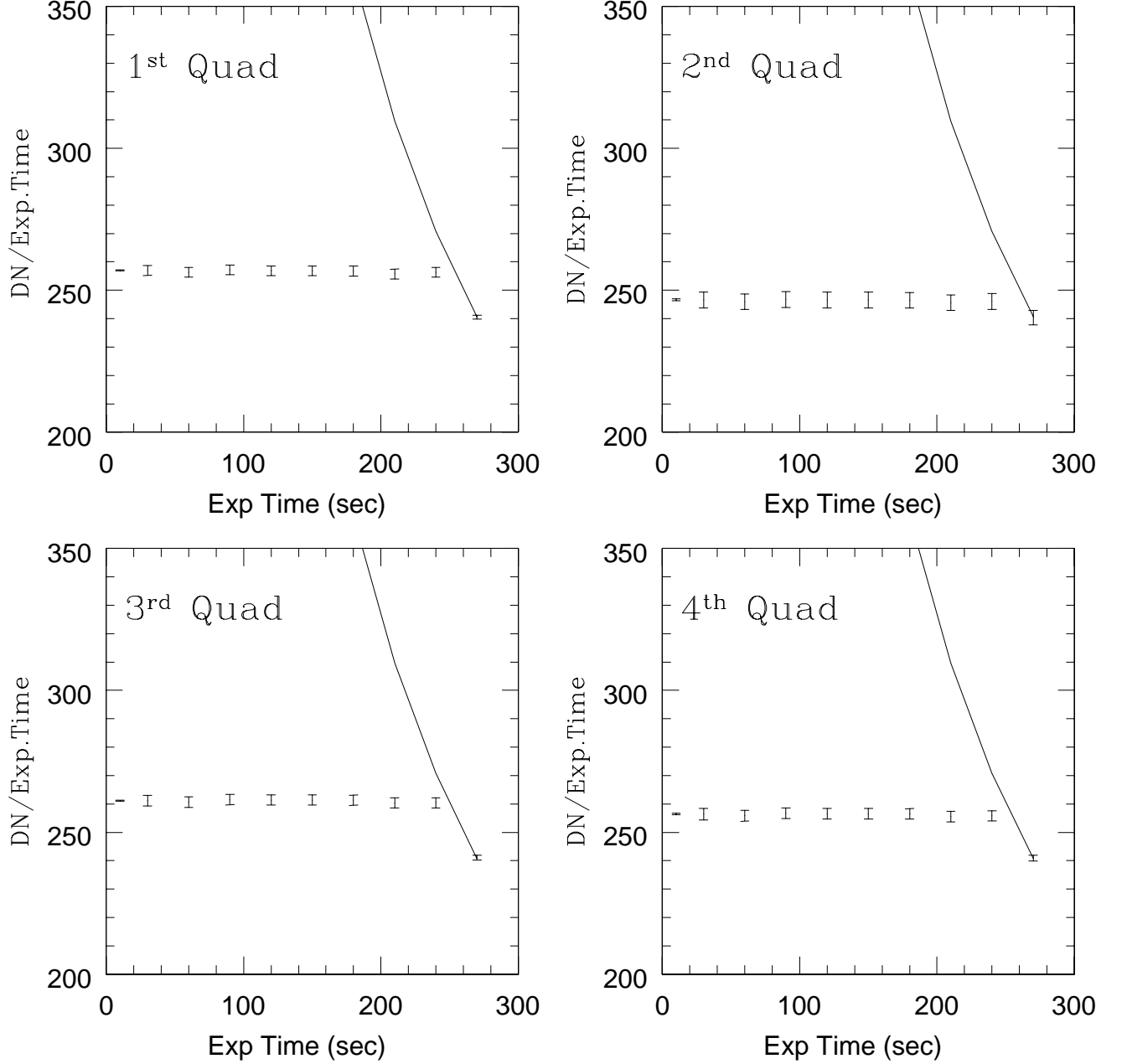


Fig. 3.— Deviation from linearity as a function of exposure time for the CCD. These show the weighted averages for the same three independent tests taken during the May 2002 observing run. The solid line is the calculated 65,000 DN line. Labelling of the quadrants is the same as in Figure 2.

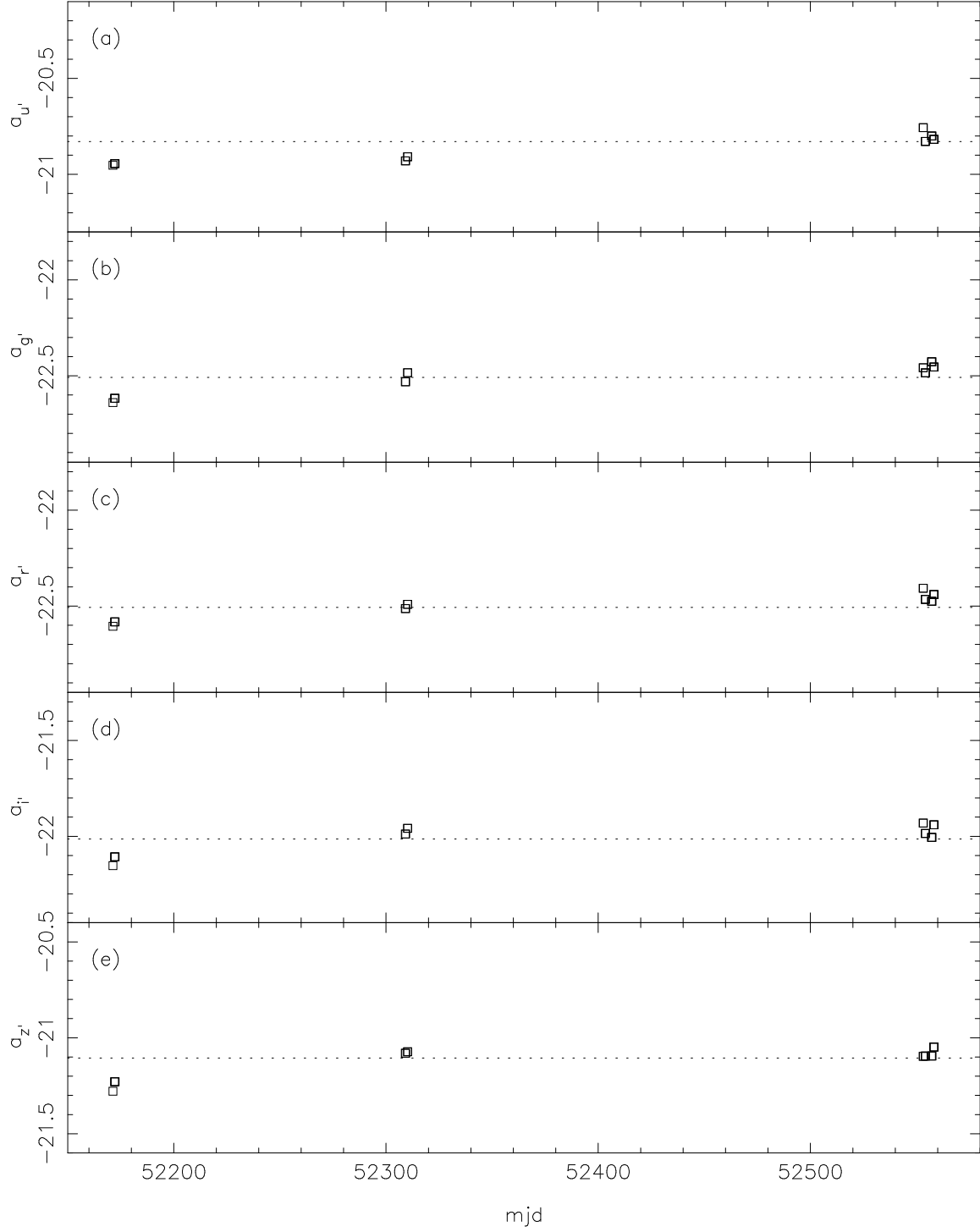


Fig. 4.— The photometric zeropoints for each night of data, by filter, $u'g'r'i'z'$, from top to bottom. The dotted line indicates the mean zeropoints. Note the slight degradation of telescope throughput with time. These values were taken from Table 3.

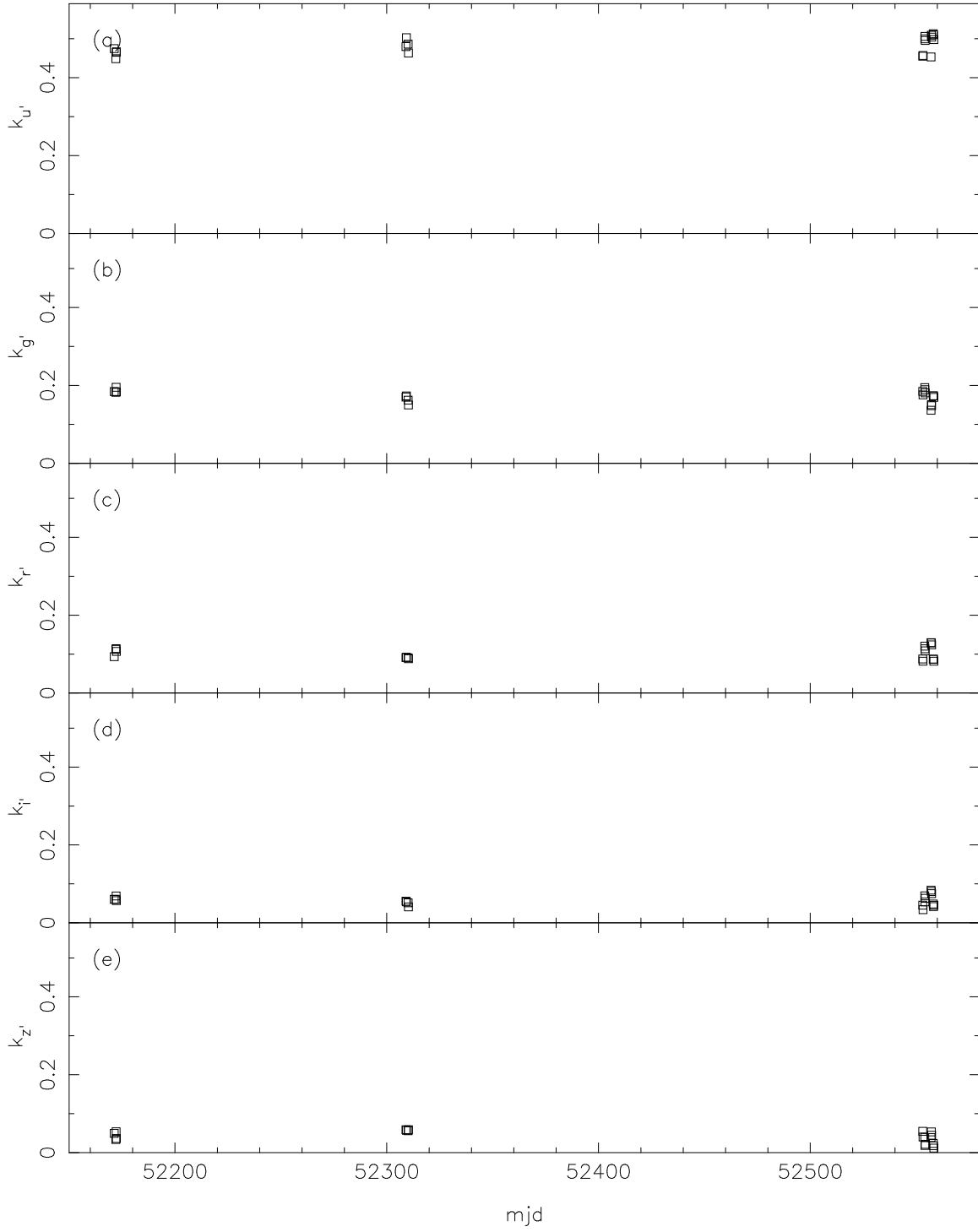


Fig. 5.— The first order extinction coefficients for each reduction block by filter, $u'g'r'i'z'$, from top to bottom. These values were taken from Table 3.

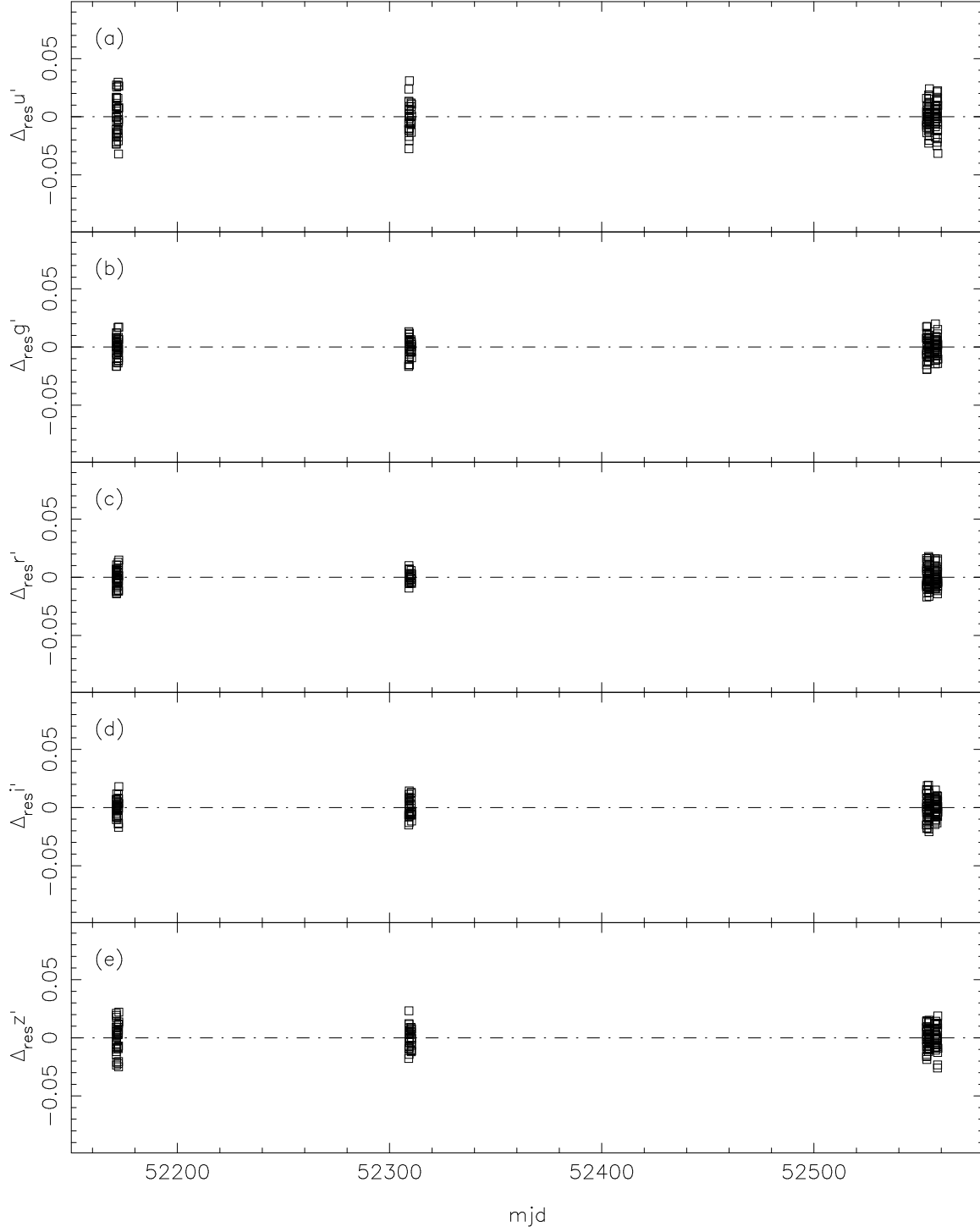


Fig. 6.— The residuals of the `excal` solution for the standard stars used in the reductions by filter, $u'g'r'i'z'$, from top to bottom. These are plotted in the sense of (observed–standard) for each night’s solution.

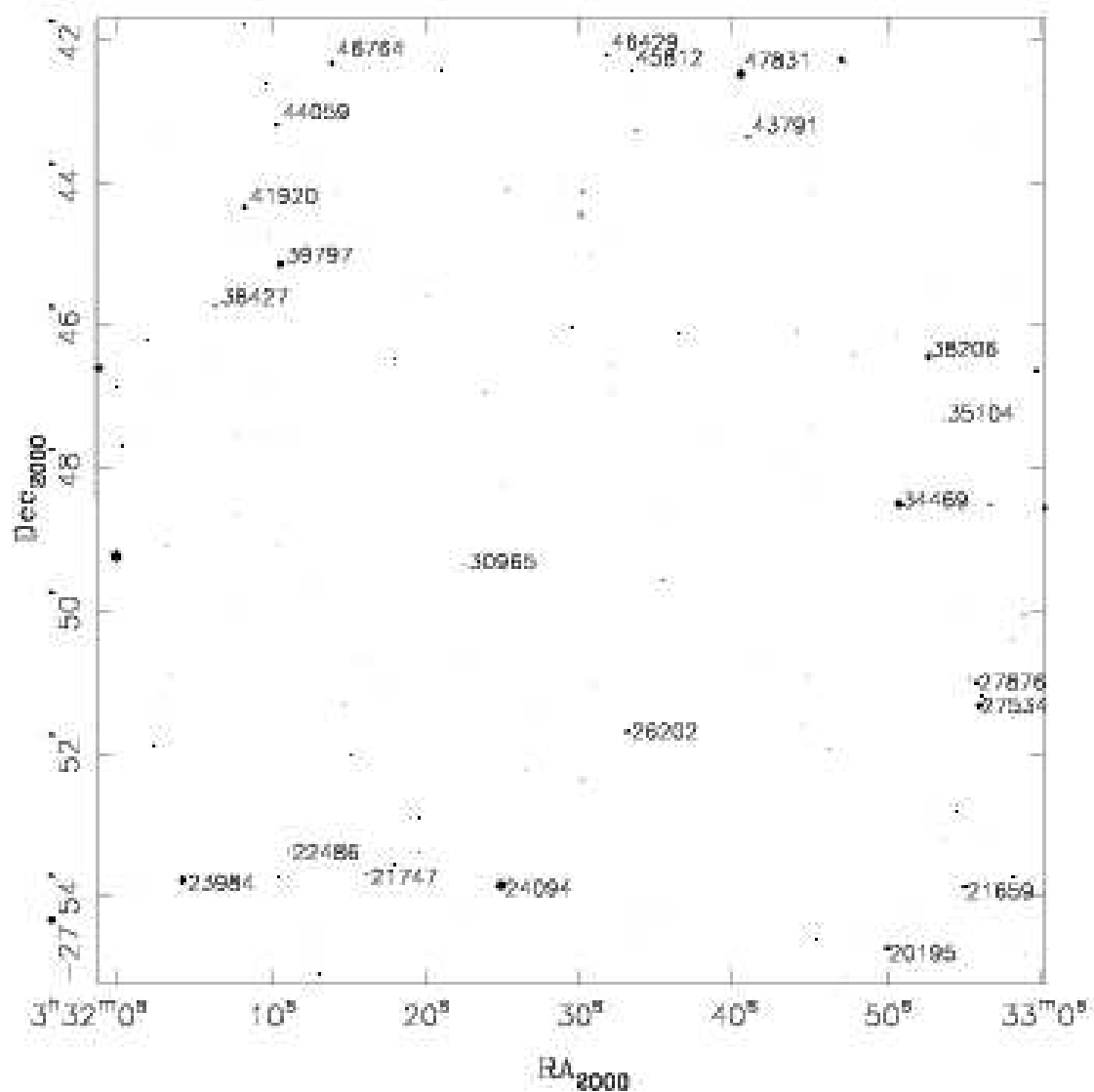


Fig. 7.— Finder chart for the CDF-S field, an r' band image. The marked stars are those selected to act as local standards. The numbers are the COMBO-17 star designations from Table 4. Coordinates for the center of the field are $\alpha = 03:32:28$, $\delta = -27:48:30$, J2000.

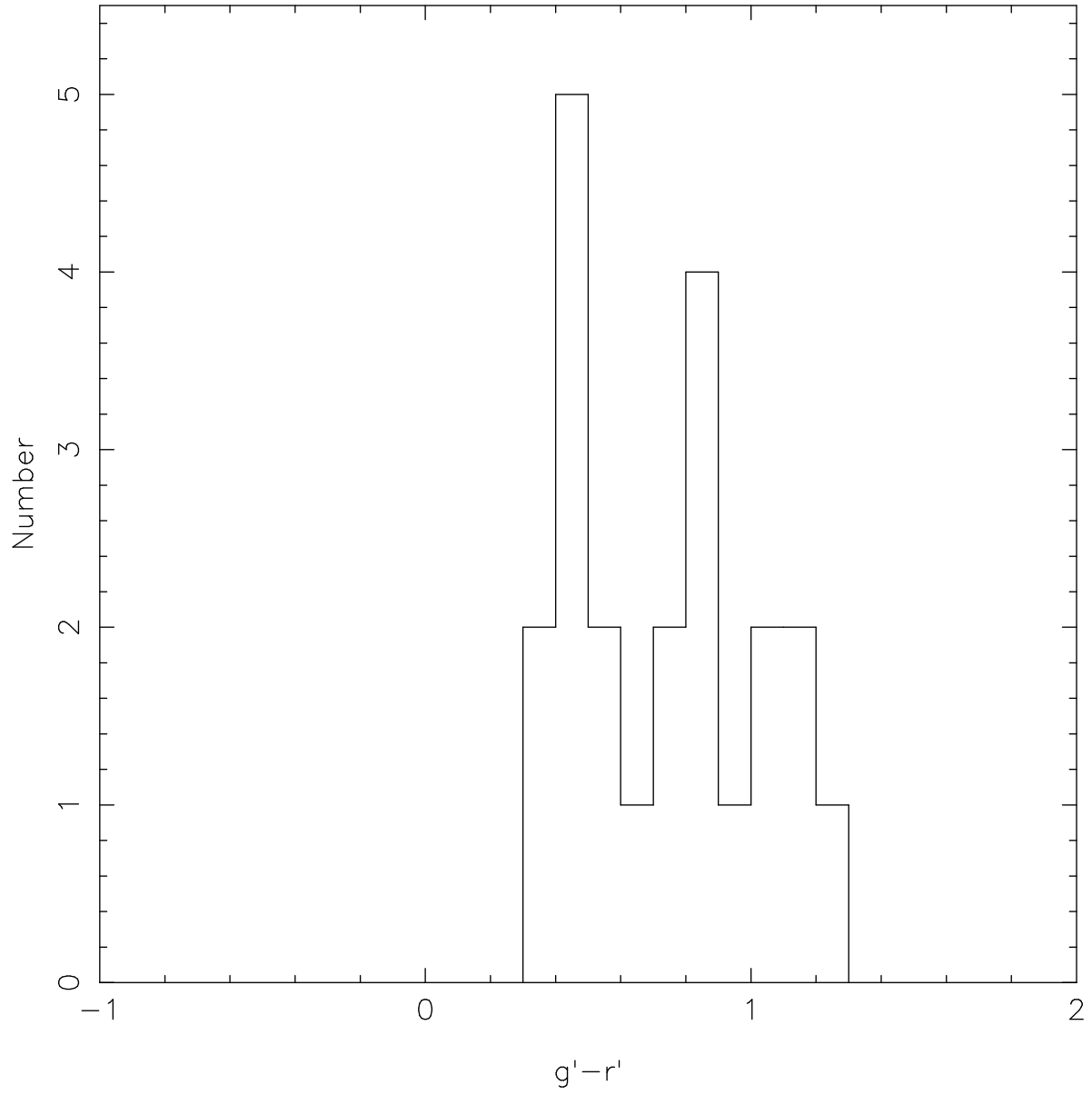


Fig. 8.— The $(g' - r')$ color distribution of local standards in the CDF-S field.

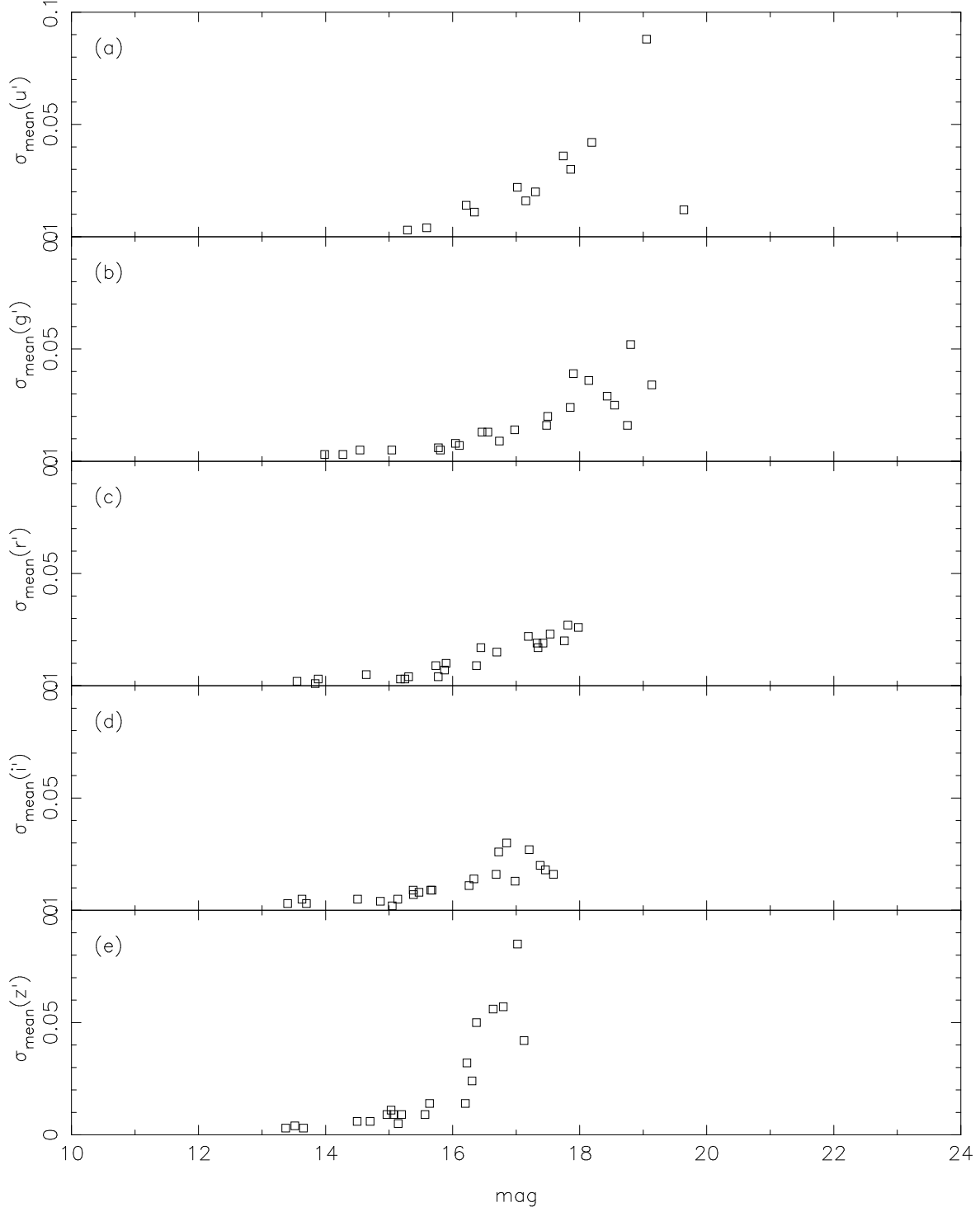


Fig. 9.— The estimated rms error in the calibrated magnitudes for the local standards in the CDF–S field versus magnitude: (a) $\sigma_{\text{mean}}(u')$ vs. u' , (b) $\sigma_{\text{mean}}(g')$ vs. g' , (c) $\sigma_{\text{mean}}(r')$ vs. r' , (d) $\sigma_{\text{mean}}(i')$ vs. i' , and (e) $\sigma_{\text{mean}}(z')$ vs. z' . These values were taken from Table 4.

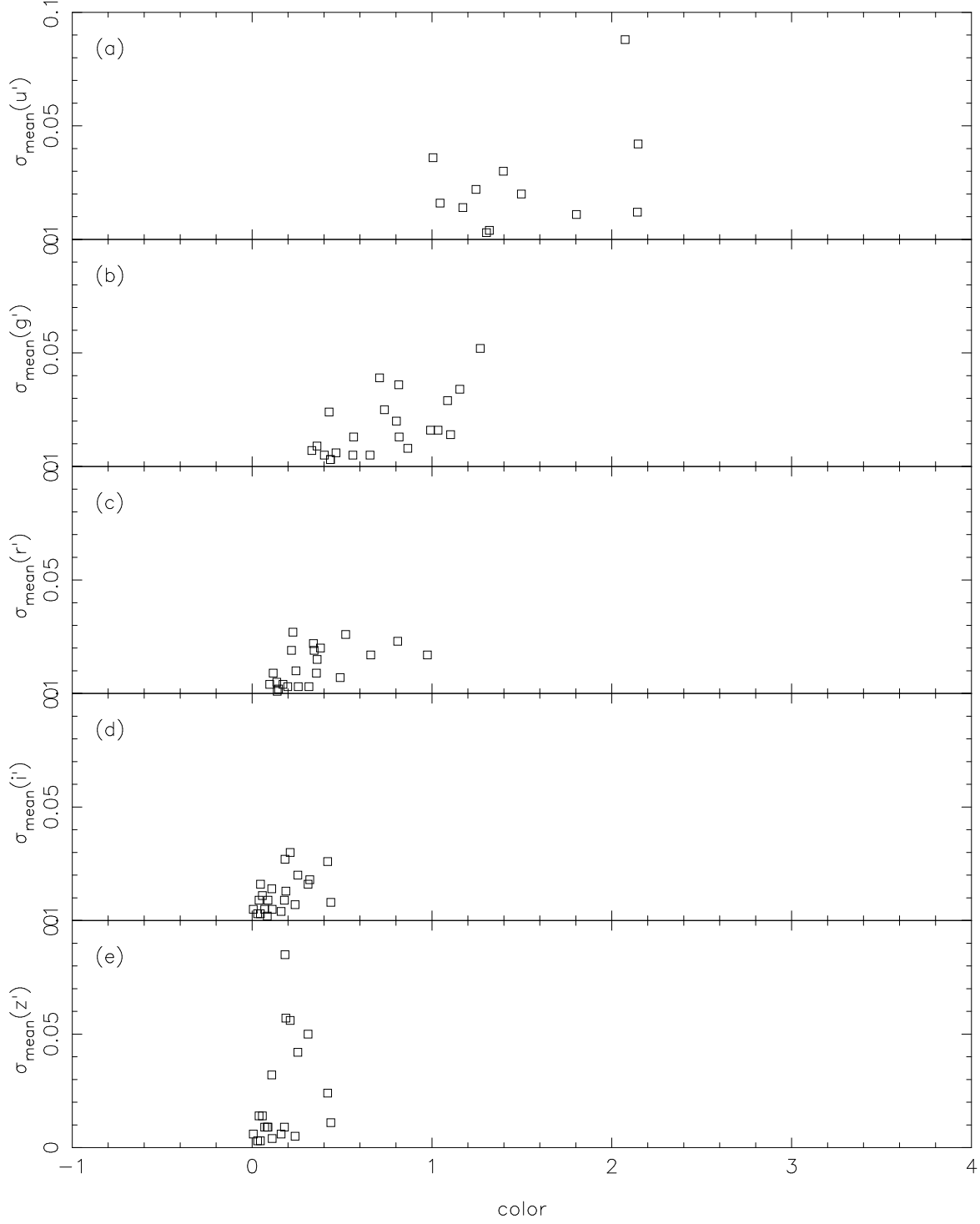


Fig. 10.— The estimated rms error in the calibrated magnitudes for the local standards in the CDF–S field versus magnitude: (a) $\sigma_{\text{mean}}(u')$ vs. $(u' - g')$, (b) $\sigma_{\text{mean}}(g')$ vs. $(g' - r')$, (c) $\sigma_{\text{mean}}(r')$ vs. $(r' - i')$, (d) $\sigma_{\text{mean}}(i')$ vs. $(i' - z')$, and (e) $\sigma_{\text{mean}}(z')$ vs. $(i' - z')$. These values were taken from Table 4.